Removal of ammonia-nitrogen in wastewater using a novel poly ligand exchanger-Zn(II)-loaded chelating resin

Yan Chen, Wei Chen, Quanzhou Chen, Changhong Peng, Dewen He and Kanggen Zhou

ABSTRACT

In this study, a novel poly ligand exchanger-Zn(II)-loaded resin was designed to effectively remove ammonia-nitrogen (NH_3-N) from wastewater. The surface morphology and structure of the Zn-loaded resin were characterized using scanning electron microscopy-energy dispersive spectroscopy (SEM-EDS) and Fourier transform infrared spectroscopy (FTIR), respectively. SEM shows the surfaces of the Zn(II)-loaded resin were rough and nonporous and EDS demonstrated that Zn^{2+} was loaded onto the resin successfully. In addition, the combination form of Zn(II) with NH_3-N adsorption reagent was revealed by FTIR spectra; the complex could be R-N-R-O-Zn-O-R-N-R and R-N-R-$(O\text{-}Zn)_2$. The kinetics and equilibrium of the NH_3-N adsorption onto the Zn(II)-loaded resin has been investigated. The effects of pH, reaction time, and temperature on NH_3-N removal from wastewater by Zn(II)-loaded resin were investigated, and the results showed that the maximum adsorption capacity reached 38.55 mg/g at pH 9.54 at 298 K in 240 min. The adsorption ability of the modified resin decreased with an increase in temperature. Moreover, the NH_3-N adsorption followed a pseudo-second-order kinetic process. The kinetic data demonstrated that the adsorption process might be limited by a variety of mechanisms. The study can provide the scientific foundation for the extensive application of a novel poly ligand exchanger-Zn(II)-loaded resin to remove NH_3-N from wastewater.

Key words | ammonia-nitrogen removal, adsorption kinetic, isotherm equilibrium study, Zn(II)-loaded resin

Yan Chen
Wei Chen
Quanzhou Chen
Changhong Peng
Dewen He
Kanggen Zhou (corresponding author)
School of Metallurgy and Environment,
Central South University,
Changsha 410083,
China
E-mail: *zhoukg63@163.com*

INTRODUCTION

The ammonium ion is the most prevalent inorganic form of nitrogen, which is present in surface water and is part of a variety of biochemical and physicochemical processes. Toxic NH_3 molecules appear only in water with high pH, temperature and in the presence of ammonium. NH_3-N originates from industrial wastewater, municipal sewage and agricultural wastes or is decomposed from organic nitrogen compounds in those wastewaters and wastes. High concentration NH_3-N could cause damage to aqueous ecosystems and even humans (Sareer *et al.* 2015). Therefore, effective removal of NH_3-N from wastewater is significantly important, and tremendous efforts have been spent on developing techniques to remove NH_3-N from aqueous solution.

Current methods for NH_3-N removal include precipitation (Chen *et al.* 2013), biological processes (Tang *et al.* 2013, 2017), ion exchange (Wirthensohn *et al.* 2009), adsorption (Babou and Hamoudi 2014), electrochemical technology (Mook *et al.* 2012), and stripping (Yuan *et al.* 2016). Biological treatment requires long retention time and has low removal efficiency in winter-time. Electrochemical technologies such as electrochemical reduction are less efficient in removing ammonium. Compared with other techniques, the adsorption method is considered as a promising technology for the treatment of NH_3-N wastewater because of its simple and effective process, lower operating cost, and economical and practical properties. Conventional adsorbents, including activated carbon, various zeolites, bentonite, and fly ash are inert for NH_3-N removal (Halim *et al.* 2010). In recent years, NH_3-N removal by adding struvite ($MgNH_4PO_4{\cdot}6H_2O$, magnesium ammonium phosphate, MAP) (Peng *et al.* 2017) has received extensive attention because of excellent solid-liquid separation performance. However, the key problem that needs to be resolved is how to reduce the treatment cost of MAP precipitation for the application of this process in

doi: 10.2166/wst.2019.020

the engineering treatment of NH_3-N-containing solutions. For example, if treatment conditions are not controlled properly, it can result in the formation of byproducts such as $Mg_3(PO_4)_2$ and $Mg(OH)_2$. In the past decade, the field of adsorption has seen the emergence of a new class of materials called metal-organic frameworks (MOFs) (Doonan *et al.* 2010). These compounds are formed by the self-assembly of metal ions, acting as coordination centers, and polyatomic organic bridging ligands (James 2003). This results in the formation of highly porous crystalline solids (James 2003). Owing to the diversity of their metallic centers and organic functionalities, one can tailor materials with specific pore shape, size, volume and chemistry (James 2003). Despite the large enthusiasm surrounding the MOFs, only a few research groups started to investigate their use for NH_3-N removal (Doonan *et al.* 2010; Saha & Deng 2010). Moreover, the potential instability of MOFs on NH_3-N adsorption at ambient conditions is scarcely addressed in the literature.

Ligand exchange technologies (Mustafa *et al.* 1998) have been widely used for removing anions or organic neutral ligands in solution. There are very few reports (Chen *et al.* 2017) on the use of ligand exchange technology to remove NH_3-N from domestic or industrial wastewater. In the field of ligand separation, highly-concentrated NH_3-N was commonly used as the effluent to exchange other ligands in ligand exchange resin. Typical 'ligand exchange' reactions can be described as follows:

$$\overline{\text{R-Zn(OH}^-\text{Na}^+)_x} + x\text{NH}_4^+ \rightarrow \overline{\text{R-Zn(OH-NH}_4^+)_x} + x\text{Na}^+ \rightarrow \overline{\text{R-Zn(NH}_3)_x} + x\text{H}_2\text{O} + x\text{Na}^+ \quad (1)$$

$$\overline{\text{R-Zn}} + x\text{NH}_3 \rightleftarrows \overline{\text{R-Zn(NH}_3)_x} \quad (2)$$

Therefore, the main objective of this work is to develop a novel poly ligand exchanger-Zn(II)-loaded chelating resin for the removal of NH_3-N in aqueous solution. For this purpose, the preparation and characterization of the modified resin were carried out. Specifically, the optimum adsorption conditions and possible adsorption mechanisms were explored using isotherm equations and kinetic models.

MATERIALS AND METHODS

Materials

The anion exchange resin used in this work was purchased from Shanghai Huizhu Resin Company, China. Because of its weak iminodiacetate functional group, small size and microporous structure, the original resin was readily modified by a zinc solution prepared using analytical-grade $ZnSO_4{\cdot}7H_2O$. After loading, the resin exhibited high removal efficiency for NH_3-N. The physical properties of the resin are shown in Table S1 (Supplementary Material, SM, available with the online version of this paper). The virgin resin has a specific surface area of 13.60 m^2/g and an average diameter of pores of 513 nm. All chemicals were of analytical grade and were purchased from Xilong Chemical Co., Ltd, China. Two NH_4Cl stock solutions were prepared by dissolving NH_4Cl solids into 1.0 g cations/L and 10 g cations/L, respectively. Deionized water was used throughout the experiments.

Preparation of Zn(II)-loaded resin

The virgin resin was washed extensively with distilled water to remove non-adhesive impurities and small particles, and then dried at 398 K for 24 hr to remove moisture. 500 mL of dried resin was filled into an exchange column, then washed slowly with saturated $ZnSO_4$ solution until the effluent had the same zinc concentration as the initial solution to ensure that the Zn(II)-loaded resin was saturated. Afterwards, the resin was washed rapidly by deionized water until the effluent zinc concentration was below 0.5 mg/L. After washing, the resin was dried at 398 K for 24 hr.

Equilibrium experiments

The sorption of NH_3-N onto Zn(II)-loaded resin was investigated in 120 mL batch reactors. Each batch reactor was filled with 1 g of Zn(II)-loaded resin and NH_3-N solution with concentrations ranging from 50 to 4,000 mg/L. The mixture was placed in a SHZ-82A temperature-controlled water-bath oscillator at 200 rpm for 10 hr. In addition, the effect of solution pH on the adsorption capacity of the Zn(II)-loaded resin was also investigated at pH values 3.10, 3.68, 5.49, 6.32, 7.00, 8.02, 9.03, 9.54, 10.48, 11.31, and 11.96 at 298 K. The pH of the solution was adjusted by 0.1 mol/L HCl and 1.0 mol/L NaOH.

The NH_3-N removal efficiency (%)R was calculated by Equation (3). The amount of NH_3-N retained in the Zn(II)-loaded resin was calculated by Equation (4) as the difference between the amounts in the initial NH_3-N solution and that remaining in the solution:

$$R\% = (C_0 - C_e)/C_0 \times 100 \quad (3)$$

$$Q_e = (C_0 - C_e) \times V/m \quad (4)$$

where R is the NH_3-N removal efficiency(%); C_0 and C_e are the initial concentration and the equilibrium concentration of NH_3-N in solution (mg/L), respectively; V is the solution volume (L); and m is the mass of the Zn(II)-loaded resin (Biškup & Subotić 2004).

Equilibrium experiments for NH_3-N removal were carried out in the batch system at 298 K, 313 K, 333 K with an accurately known amount of 1 g of Zn(II)-loaded resin sample equilibrated with 100 mL of ammonium solution in the reactor.

Kinetic studies

The experimental data obtained in batch experiments at various initial concentrations of NH_3-N were further analyzed using kinetics modeling. Also, additional experiments were performed using three different initial concentrations of 50, 100 and 200 mg/L, to verify data obtained by proposed generalized predictive model. The amount of NH_3-N retained in the Zn(II)-loaded resin, Q_t, was calculated by Equation (5) as the difference between the amounts present in the initial NH_3-N solution and that remaining in the solution:

$$Q_t = (C_0 - C_t) \times V/m \tag{5}$$

where C_0 and C_t are the initial concentration and equilibrium concentration at time t of NH_3-N in solution (mg/L), respectively; V is the volume of solution(L); and m is the mass of the Zn(II)-loaded resin.

Analytical methods

The pH of the solutions was measured using a Mettler Toledo 320 pH meter. The resin was dried in a 101 electric blast-drying oven. The NH_3-N and Zn^{2+} concentrations were determined by using Nessler reagent and zinc reagent with a VIS-7220 spectrophotometer. The resins that were immersed in different solutions were all shaken in a SHZ-82A water-batch constant temperature oscillator. The surface morphology and chemical composition of the resin were characterized using scanning electron microscopy-energy dispersive spectroscopy (SEM-EDS) (Hitachi Zeeman Z-8200, Japan). Chemical structure of the resin was analyzed using a Fourier transform infrared (FTIR) spectrometer (Thermo Nicolet Company 380, USA) equipped with a DTGS detector with a spectral resolution of 4 cm^{-1}. Each FTIR spectrum was an average of 64 scans.

RESULTS AND DISCUSSION

Preparation and characteristics of Zn(II)-loaded resin

The Zn(II)-loaded resin was successfully prepared, and the scheme of preparation and adsorption is shown in Figure 1. First, Zn(II)-loaded resin was prepared by replacing Na^+ ions on the original resin with Zn^{2+}. Then NH_3-N in the solution was adsorbed onto the Zn(II)-loaded resin surface and reacted with Zn to form the complexes. The surface morphologies of the virgin and Zn(II)-loaded resin were characterized by SEM-EDS analysis (Figure 2), and EDS

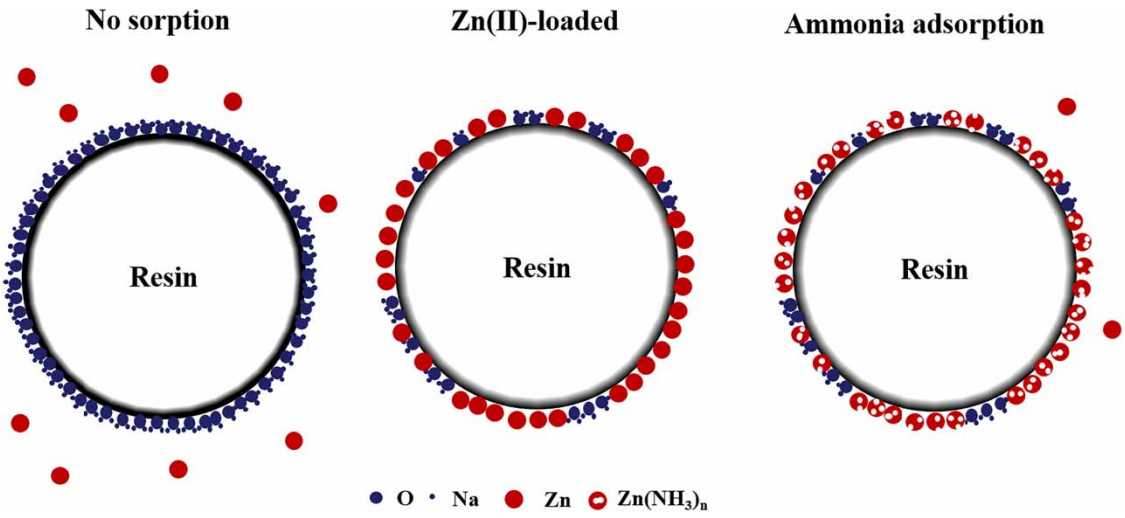

Figure 1 | Preparation route of Zn(II)-loaded resin.

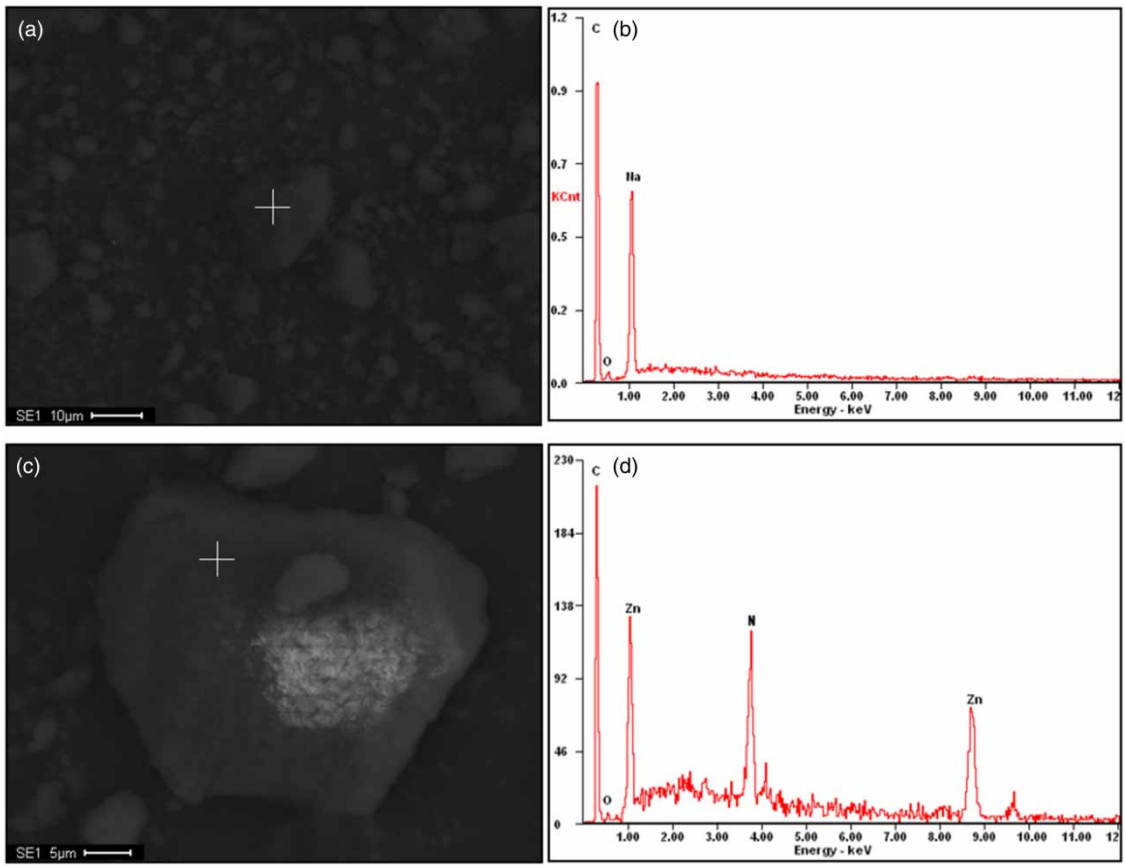

Figure 2 | SEM and energy spectrum of Zn(II)-loaded resin: (a) SEM image of virgin resin; (b) EDS spectrum of virgin resin; (c) SEM image of Zn(II)-loaded resin; (d) EDS spectrum of Zn(II)-loaded resin.

results (Figure 2(b) and 2(d)) demonstrated that Zn^{2+} was loaded onto the resin successfully. As shown in Figure 2(c), the surfaces of the Zn(II)-loaded resin were rough and nonporous. In addition, the Brunauer-Emmett-Teller (BET) results suggested that the zinc load doubled the specific surface area of the resin (Table S2, available online).

Figure 3(a) shows the FTIR spectra of virgin, Zn-loaded, and NH_3-N adsorbed resins. There was a peak shift for the C = O bond in the infrared spectrum after zinc loading as well as after NH_3-N adsorption (from 1,591 cm^{-1} to 1,605 cm^{-1} and 1,600 cm^{-1}) and the band corresponding to the C–O stretching also shifted from 984 cm^{-1} to 1,013 cm^{-1} (Wang *et al.* 2014; Guan *et al.* 2018) (Figure 3(a)). The intensity of C = O was weakened after loading with zinc, suggesting the formation of coordinated covalent bond between Zn and carboxylic groups in the resin. In addition, after Zn modification, peak intensity at 1,326 cm^{-1} decreased, while that at 1,500 cm^{-1} showed a slight increase, which could be attributed to the transformation of monodentate to bidentate and bridging (Mustafa *et al.* 1997) (Figure 3(b)). After NH_3-N adsorption, the peak of the C=O bond further shifted from 1,605 cm^{-1} to 1,600 cm^{-1} and two new bands appeared at 533 cm^{-1} and 475 cm^{-1}, assigned to the stretching vibration of N–Zn and O–Zn, suggesting the involvement of $-NH_2$ and –COO– groups during adsorption (Sun & Wang 2006).

Effect of pH on Zn(II)-loaded resin exchange performance

pH is one of the most critical controlling parameters in ammonium removal by Zn(II)-loaded resin, since it can influence both the characters of the exchanging ions and the resin itself. In order to investigate the effect of pH on the adsorption of NH_3-N by Zn(II)-loaded resin, 1 g of modified resin was added into 100 mL of NH_3-N solution (100 mg/L). Experiments were performed in the pH range of 3.00–12.00 and the solutions were shaken for 10 hr at 200 rpm speed. All possible reactions and species involved in the system are presented in Table S4 (available online),

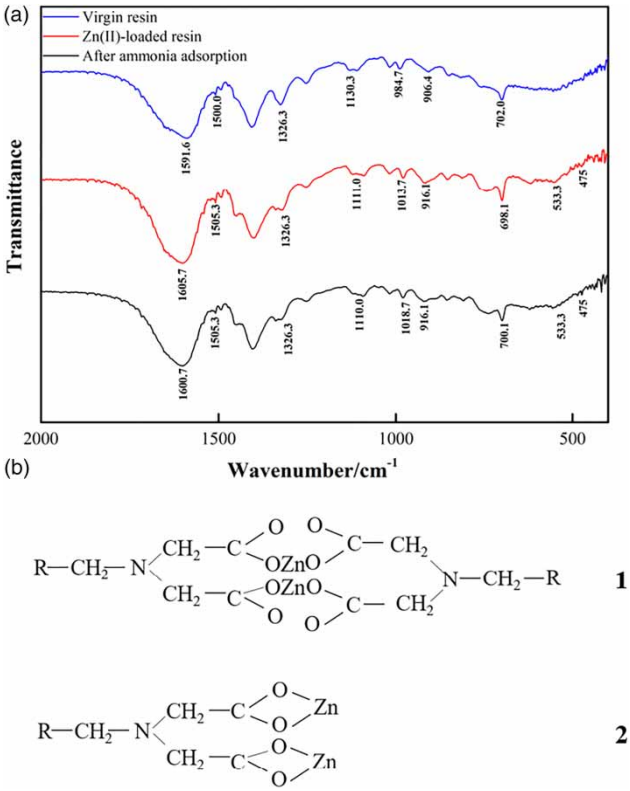

Figure 3 | (a) FTIR spectra of virgin resin (blue line), Zn-loaded resin (red line) and Zn-loaded resin after NH_3 adsorption (black line), (b) possible structure of metal-carboxylate complexes. The full color version of this figure is available in the online version of this paper, at http://dx.doi.org/10.2166/wst.2019.020.

which could be used to calculate the concentration distribution of each species under various pH values. Using the Academic Software (UK, http://www.acadsoft.co.uk), the content distributions of Zn^{2+} and NH_3-N species with pH are calculated and presented in Figure 4. The effect of solution pH on the sorption process of ammonium is shown in Figure 5.

NH_3-N in aqueous solution exists in two forms, un-ionized (NH_3) and ionized (NH_4^+). The fraction of these two forms of NH_3-N changes with the change of solution pH value. As shown in Figure 4, at pH values lower than 6.50, stably ionized NH_4^+ exists predominantly in aqueous solution. At pH values from 6.50 to 12.00, un-ionized (NH_3) increased sharply with the increase of solution pH. Moreover, in this pH range, NH_3-N could easily react with Zn^{2+} to form $Zn(NH_3)_n^{2+}$. At pH values higher than 8.00, the formation of $Zn(NH_3)_4^{2+}$ became prominent.

As shown in Figure 5, at low pH values (ranging from 3.00 to 7.00), the NH_3-N removal efficiency hardly changed with solution pH, and the overall removal efficiency was below 7.0%. In the pH range between 7.00 and 9.54, the removal efficiency increased sharply from 6.6% to 35.4%

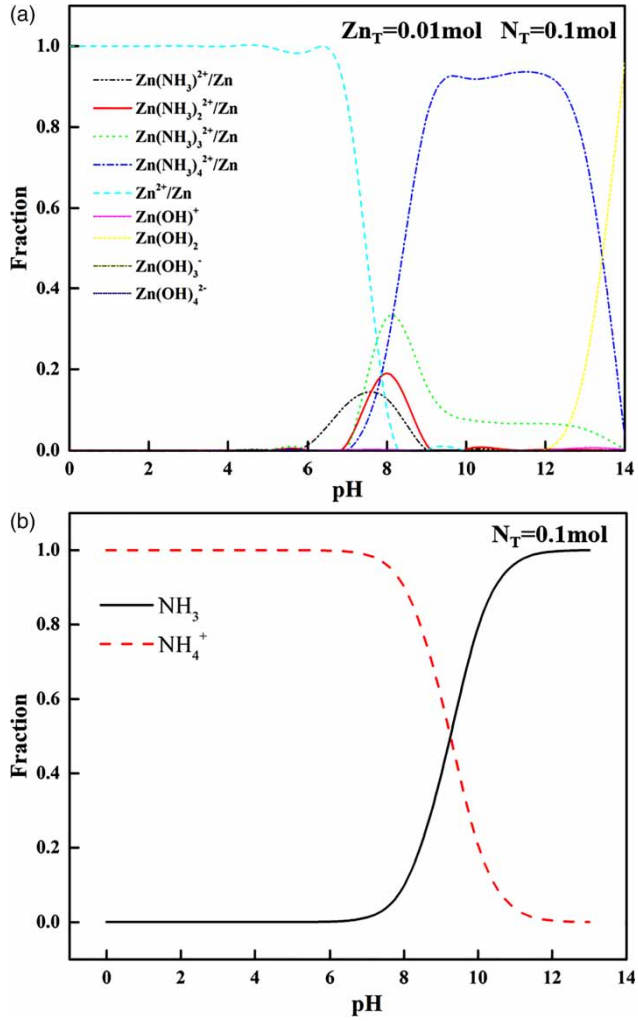

Figure 4 | Distribution of Zn^{2+} (a) and NH_4^+ (b) species under various pH values (equilibrium constants obtained from Lange and Dean (2005)).

with the increase of solution pH. According to the result in Figure 4, in this pH range Zn^{2+} could react with NH_3 to form $Zn(NH_3)_n^{2+}$. Above pH 9.54, the NH_3-N removal efficiency decreased with increasing solution pH. Simultaneously, a sharp increase in the OH^- concentration may result in forming the unexpected precipitate $Zn(OH)_2$ and lead to the decrease of Zn(II) loaded on the resin. Hence, the NH_3-N removal efficiency was the highest at a pH value around 9.54.

NH_3-N adsorption isotherms

The salient features of adsorption isotherms are necessary to optimize the design of an adsorption system for the adsorption of adsorbate. The dynamic adsorptive separation of the solute from the solution onto the adsorbent depends upon a

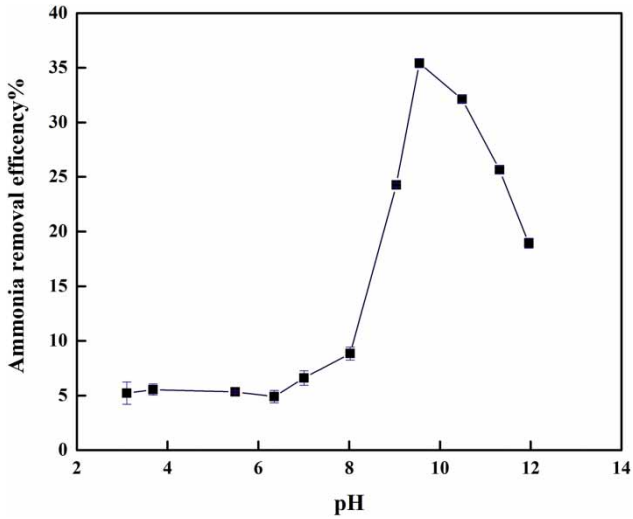

Figure 5 | Effect of pH on the ammonium removal efficiency of Zn(II)-loaded resin (operating conditions: initial NH_3-N concentration, 100 mg/L; resin dosage, 1 g/100 mL; agitation period, 10 hr).

good description of the equilibrium separation between the two phases. Various models have been proposed and applied to explain the equilibrium characteristics of adsorption. However, the most important factor is to have the applicability over the entire adsorption process. The most widely used isotherm models for solid-liquid adsorption are the Langmuir, Freundlich, Temkin, and Redlich-Peterson isotherms. The parameters of all reaction-based models were calculated using nonlinear regression analysis.

Langmuir isotherm

The Langmuir isotherm describes a monolayer adsorption based on the active sites within the adsorbent. It is given as:

$$Q_e = Q_m C_e K_L/(1 + C_e K_L) \quad (6)$$

where C_e is the equilibrium concentration of NH_3-N in solution (mg/L), Q_e is the amount of adsorbate at equilibrium per unit mass sorbent (mg/g), Q_m is the maximum monolayer adsorption capacity (mg/g), and K_L is the Langmuir adsorption constant (1/g).

Figure 6(a) shows the plots of Q_e against C_e at three temperatures for the fitting of the Langmuir isotherm model. The Langmuir constants were calculated from the plots and are summarized in Table 1. The maximum monolayer adsorption capacities obtained from the Langmuir plots at 298 K, 313 K and 333 K were 38.55, 33.66 and 24.98 mg/g, respectively. The NH_3-N adsorption capacity on Zn-loaded resin increased with the increase of initial

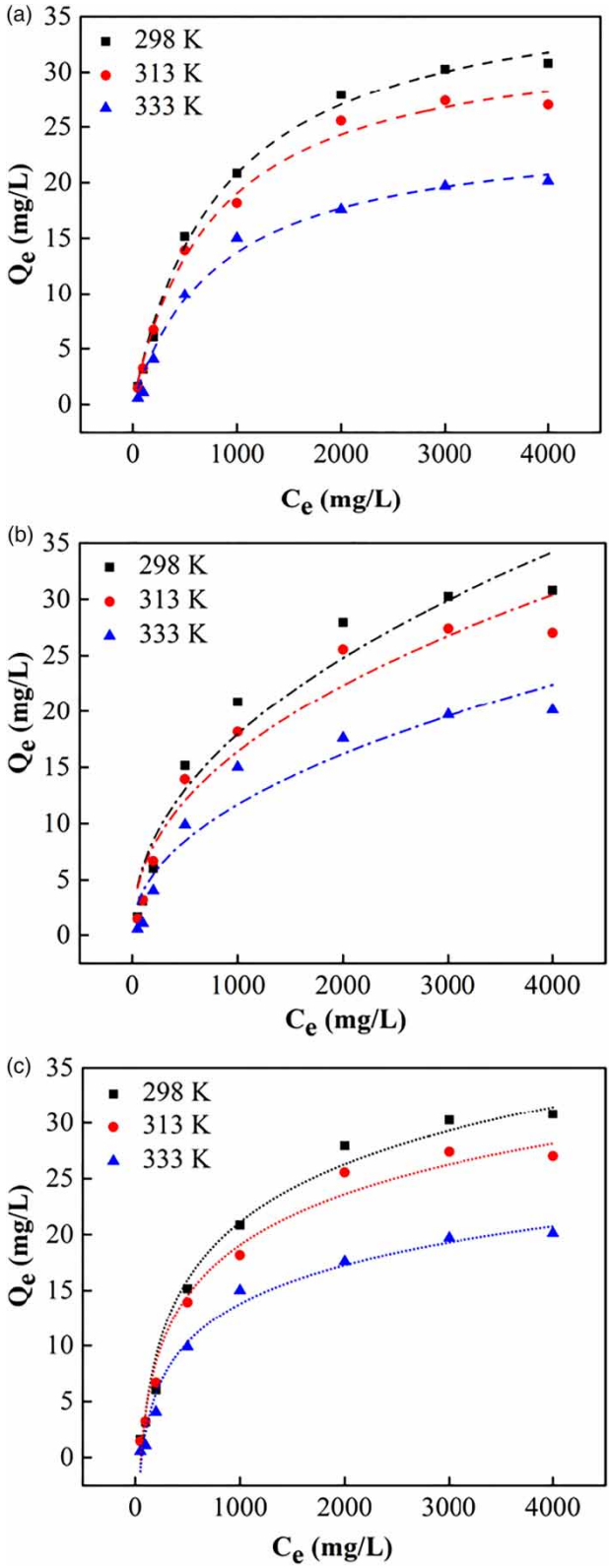

Figure 6 | Langmuir (a), Freundlich (b) and Temkin (c) isotherm plots for the adsorption of NH_4^+ at various temperatures (operating conditions: initial NH_3-N concentration, 100 mg/L; resin dosage, 1 g/100 mL).

Table 1 | Isotherm parameters of NH_3-N uptake on the Zn(II)-loaded resin

Isotherm	Adsorbent	Q_m(mg g^{-1})	K_L(L mg^{-1})	R^2
Langmuir	Zn(II)-loaded resin 298 K	38.55	0.0012	0.995
	Zn(II)-loaded resin 313 K	33.66	0.0013	0.992
	Zn(II)-loaded resin 333 K	24.98	0.0012	0.986
	Natural zeolite (Saltalı *et al.* 2007)	9.64		
	Natural Turkish clinoptilolite (Karadag *et al.* 2006)	8.121		
	Clinoptilolite (Zhu & Ni 2009)	15.44		
	Sardinian natural zeolites (Cincotti *et al.* 2001)	8.15(raw) 12.26 (Na-zeolite)		
Isotherm	**Adsorbent**	K_F	n	R^2
Freundlich	Zn(II)-loaded resin 298 K	0.7262	2.15	0.945
	Zn(II)-loaded resin 313 K	0.7560	2.24	0.943
	Zn(II)-loaded resin 333 K	0.4612	2.136	0.924
Isotherm	**Adsorbent**	K_T (L mg^{-1})	B	R^2
Temkin	Zn(II)-loaded resin 298 K	0.0169	7.46	0.978
	Zn(II)-loaded resin 313 K	0.0184	6.55	0.981
	Zn(II)-loaded resin 333 K	0.0156	5.11	0.979

NH_3-N concentrations in solutions and decreased with the increase of solution temperature, suggesting that the NH_3-N adsorption process might be an exothermic reaction.

The essential characteristics of the Langmuir isotherm have been described by the dimensionless separation factor or equilibrium constant, R_L, which is defined as:

$$R_L = 1/(1 + K_L C_0) \tag{7}$$

The R_L value indicates the shape of the isotherm to be either unfavorable ($R_L > 1$), linear ($R_L = 1$), favorable ($0 < R_L < 1$), or irreversible ($R_L = 0$). The calculated values of R_L at different initial concentrations of NH_3-N were all below 1.0, confirming that the adsorption of ammonium was a favorable process.

Freundlich isotherm

The Freundlich isotherm is derived by assuming a heterogeneous surface (multilayer adsorption) with a non-uniform distribution of heat of adsorption over the surface. This isotherm assumes that the adsorption sites are distributed exponentially with respect to the heat of adsorption and is expressed as:

$$Q_e = K_F C_e^{\frac{1}{n}} \tag{8}$$

where K_F and n relate to the multilayer adsorption capacity and intensity of adsorption, respectively. n is also known as the heterogeneity factor. The Freundlich isothermal plots of NH_3-N adsorption are presented in Figure 6(b), and the coefficients are shown in Table 1. The values of $1/n$ were lower than 1 at all temperatures, further indicating that the adsorption was favorable (Vasiliu *et al.* 2011).

Temkin isotherm

The Temkin isotherm assumes that the effects of the heat of adsorption of all the molecules in the layer decreases linearly with coverage due to adsorbent–adsorbent interactions. The adsorption is characterized by a uniform distribution of the binding energies up to maximum binding energy. The Temkin isotherm equation is given as:

$$Q_e = B \bullet \ln (K_T \bullet C_e) \tag{9}$$

where K_T is the equilibrium binding constant (L/g) corresponding to the maximum binding energy and the constant B is related to the heat of adsorption. The isotherm constants K_T and B can be calculated from the fitting curve of Q_e versus C_e (Figure 6(c)). The calculated values of K_T and B are shown in Table 1 along with the correlation coefficient value.

As shown in Table 1, the superior regression coefficients for the Langmuir model compared to the Freundlich model suggested that the adsorption process was monolayer. The Langmuir values of R_L below 1.0 and Freundlich values of $1/n$ between 0.446 and 0.645 ($0 < 1/n < 1$) revealed the favorability of the adsorption of NH_4^+ onto Zn(II)-loaded resin.

The equilibrium studies revealed that Zn(II)-loaded resin exhibited a much higher uptake concentration of ammonium at equilibrium at 298 K compared with those at 313 K or 333 K. According to the thermodynamic calculation (detailed in SM, Table S3, available online), the adsorption process was an exothermic reaction. Therefore, increasing temperature could result in a decrease in ammonium adsorption. Furthermore, as shown in Table 1, the maximum adsorption capacity reached 38.55 mg/g at 298 K, which was significantly higher than those of the natural zeolite (Saltalı *et al.* 2007), natural Turkish clinoptilolite (Karadag *et al.* 2006), clinoptilolite (Zhu & Ni 2009) and Sardinian natural zeolites (Cincotti *et al.* 2001).

NH_3-N adsorption kinetics

Adsorption kinetics analysis, an important method for describing the adsorption process, is used to interpret the transport of adsorbates inside adsorbents for real applications and plays a key role in elucidating the dominant adsorption mechanism. To describe the changes in solution of NH_3-N with time, three kinetic models of adsorption; that is, pseudo-first-order equation, pseudo-second-order equation, and intra-particle diffusion, were fitted for the NH_3-N adsorption onto Zn(II)-loaded resin. The pseudo-first-order model is one of the most widely used kinetic models for depicting the adsorption process in solution. The pseudo-second-order model was used to describe the chemisorption process (Habibul & Chen 2018). The intra-particle diffusion model assumes that intra-particle diffusion is the only rate limiting step (Zhou *et al.* 2015). Selecting the best model is significantly important to understand the behavior of the adsorbent, with different systems relating to different models. The parameters of all reaction-based models were calculated using nonlinear regression analysis.

Lagergren pseudo-first-order kinetic

The Lagergren pseudo-first-order kinetic (Chai *et al.* 2009; Wang *et al.* 2017) is one of the most widely used models for the sorption of the solute from aqueous solution. The Lagergren pseudo-first-order kinetic equation is given as:

$$dQ_t/dt = k_1(Q_e - Q_t) \tag{10}$$

where Q_t is the amount of NH_3-N adsorbed at time t (mg/g); k_1 is the Lagergren pseudo-first-order rate constant (min^{-1}), and t is the contact time (min). Q_m in Table 2 is the maximum adsorption value obtained by model fitting.

The rate constants, k_1, were found to be in the range of 0.0475–0.0722 min^{-1} at initial NH_3-N concentrations of 50–200 mg/L (Table 2). The equilibrium sorption capacity, Q_e, increased with initial concentration. However, as shown in Figure 7(a) and Table 2, although the correlation coefficients of the plots have values higher than 0.9, Q_m values obtained from the model were not consistent with experimental Q_e values. Therefore, the sorption of NH_3-N onto Zn(II)-loaded resin did not follow a pseudo-first-order mechanism.

Pseudo-second-order kinetic

The pseudo-second-order kinetic equation is given as:

$$dQ_t/dt = k_2(Q_e - Q_t)^2 \tag{11}$$

where k_2 is the pseudo-second-order rate constant (g/mg min).

The same trend, compared to the Lagergren pseudo-first-order kinetic, was observed (Table 2); that is, Q_e increased with increase in initial NH_3-N concentration, but the values were higher. The correlation coefficients R^2 were higher than that of the pseudo-first-order model (>0.983), and the calculated equilibrium sorption capacity (Q_m) was more consistent with the experimental data (Figure 7(b)). These results indicated that the adsorption of ammonium onto Zn(II)-loaded resin could be pseudo-second-order sorption. In the ammonium adsorption onto the Zn(II)-loaded resin, the ammonium was likely to form complexes with Zn on the resin surface, which was confirmed by the FTIR analyses. These results indicated that the NH_3-N adsorption on Zn-loaded resin was mostly controlled by chemisorption behavior (Zhou *et al.* 2014).

Weber-Morris diffusion model

The Weber-Morris diffusion model (Apiratikul & Pavasant 2008) is given as:

$$Q_t = k_d t^{\frac{1}{2}} + I \tag{12}$$

where I is the intercept of the vertical axis. This intercept could be employed to validate the effect of diffusion mechanisms of the solute film and intra-particle diffusion. If $I = 0$, the intra-particle diffusion is considered as the rate limiting step, while if $I > 0$, both film and intra-particle diffusion are considered as the rate limiting steps.

Table 2 | Kinetic parameters for NH_3-N adsorption

Adsorbent	Q_m(mg/g)	Q_e(mg/g)	k_1(min^{-1})	R^2
Pseudo-first-order				
Zn(II)-loaded resin 50 mg/L	2.303	1.507	0.0722	0.9254
Zn(II)-loaded resin 100 mg/L	4.892	3.315	0.0475	0.9649
Zn(II)-loaded resin 200 mg/L	8.712	6.267	0.0593	0.9449
Adsorbent	**Q_e(mg/g)**	**k_2(g/mg min)**	**R^2**	
Pseudo-second-order				
Zn(II)-loaded resin 50 mg/L	1.577	0.0648	0.990	
Zn(II)-loaded resin 100 mg/L	3.486	0.0196	0.991	
Zn(II)-loaded resin 200 mg/L	6.571	0.0129	0.983	
Adsorbent	**k_t(mg/g $min^{-1/2}$)**	**C(mg/g)**	**R^2**	
Intra-particle diffusion(Step I)				
Zn(II)-loaded resin 50 mg/L	0.1014	0.03386	0.9753	
Zn(II)-loaded resin 100 mg/L	0.00445	0.05892	0.9969	
Zn(II)-loaded resin 200 mg/L	0.065	0.86	0.8799	
Intra-particle diffusion(Step II)				
Zn(II)-loaded resin 50 mg/L	7.72×10^{-4}	1.2752	0.9592	
Zn(II)-loaded resin 100 mg/L	1.48×10^{-3}	2.8744	0.9326	
Zn(II)-loaded resin 200 mg/L	3.13×10^{-3}	5.401	0.9453	
Intra-particle diffusion(Step III)				
Zn(II)-loaded resin 50 mg/L	1.51×10^{-6}	1.586	0.1035	
Zn(II)-loaded resin 100 mg/L	6.94×10^{-6}	3.399	0.2849	
Zn(II)-loaded resin 200 mg/L	7.95×10^{-6}	6.47	0.3658	

The fitting result is shown in Figure 7(c), and the calculated parameters are listed in Table 2. The Weber-Morris diffusion model can be divided into three steps. The first stage could be attributed to the diffusion of NH_3-N through the solution to the external surface of Zn(II)-loaded resin and diffusion of NH_3-N through the boundary layer to the surface of Zn(II)-loaded resin. The second stage described the gradual sorption, and intraparticle diffusion was the rate-limiting factor. The third stage was attributed to the final equilibrium, for which the intraparticle diffusion started to slow down due to the extremely low concentration of NH_3-N left in solution. In general, the diffusion rates decreased with increasing contact time due to the smaller pores for diffusion, since the NH_3-N diffused into the inner structure of the Zn(II)-loaded resin. Judged from the values of R^2, the Weber-Morris model did not fit well with the experimental data, indicating that particle diffusion was not the only rate-limited step in the adsorption process. The NH_3-N adsorption process might be affected by a variety of mechanisms.

CONCLUSIONS

In the present work, a novel poly ligand exchanger-Zn(II)-loaded resin was designed for the adsorption removal of NH_3-N from wastewater. The surfaces of the Zn(II)-loaded resin were rough and nonporous, and zinc load doubled the specific surface area of the resin. After Zn(II) loading, the resin structure changed from monodentate to bidentate/bridging as suggested by the FTIR results. When compared with literature, the Zn(II)-loaded resin showed excellent performance for NH_3-N adsorption and the maximum adsorption capacity can be up to 38.8 mg/g. The adsorption of NH_3-N onto the Zn(II)-loaded resin was affected by the temperature, initial concentration and pH, while the impact of Zn(II)-loaded resin particle size was negligible. The correlation coefficients of Langmuir were higher than those of other models, indicating that the Langmuir model best describes the adsorption of NH_3-N onto Zn(II)-loaded resin. Furthermore, the adsorption of

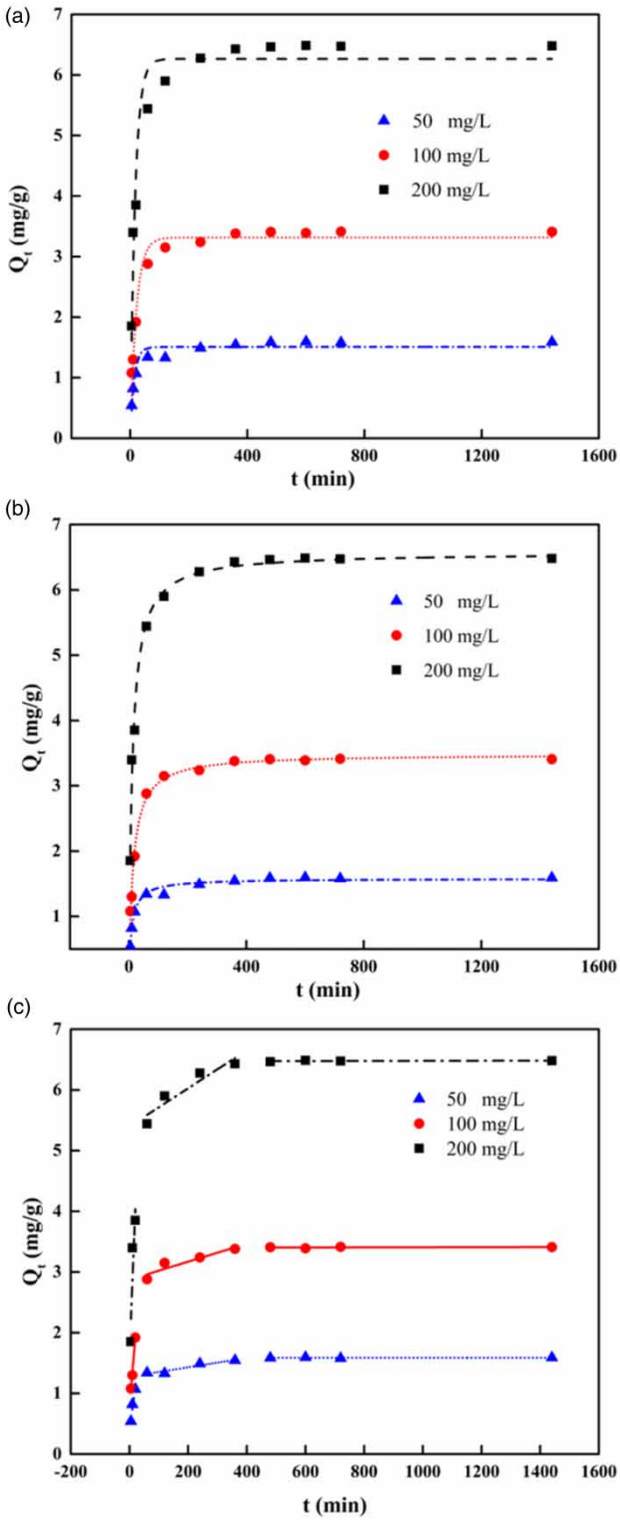

Figure 7 | (a) Pseudo-first-order, (b) pseudo-second-order and (c) intra-particle kinetic model in the adsorption of NH_3-N onto Zn(II)-loaded resin. (pH 9.54, temperature 298 K).

NH_3-N onto Zn(II)-loaded resin appeared to follow a pseudo-second-order kinetic process and was predominantly controlled by chemisorption behavior. The poly ligand exchanger-Zn(II)-loaded resin may provide an alternative for the adsorptive removal of NH_3-N nitrogen from wastewater.

ACKNOWLEDGEMENTS

The authors acknowledge the financial support from Fundamental Research Funds for the Central Universities of Central South University.

REFERENCES

Apiratikul, R. & Pavasant, P. 2008 Sorption of Cu^{2+}, Cd^{2+} and Pb^{2+} using modified zeolite from coal fly ash. *Chem. Eng. J.* **144**, 245–258.

Babou, K. R. B. & Hamoudi, S. 2014 Investigation of ammonium ion removal from aqueous solutions using arene- and propylsulfonic acid functionalized mesoporous silica adsorbents. *J. Environ. Qual.* **43**, 1032.

Biškup, B. & Subotić, B. 2004 Kinetic analysis of the exchange processes between sodium ions from zeolite A and cadmium, copper and nickel ions from solutions. *Sep. Purif. Technol.* **37**, 17–31.

Chai, L. Y., Min, X. B., Tang, N. & Wang, Y. Y. 2009 Mechanism and kinetics of Zn(II) removal from wastewater by immobilized beads of SRB sludge. *Int. J. Environ. Pollut.* **37** (1), 20–33.

Chen, Y. N., Liu, C. H., Nie, J. X., Luo, X. P. & Wang, D. S. 2013 Chemical precipitation and biosorption treating landfill leachate to remove ammonium-nitrogen. *Clean Technol. Environ.* **15**, 395–399.

Chen, Q., Zhou, K. G. & Hu, Y. 2017 Effect of competing ions and causticization on the ammonia adsorption by a novel poly ligand exchanger (PLE) ammonia adsorption reagent[J]. *Water Sci. Technol.* **75** (6), 1294.

Cincotti, A., Lai, N., Orrù, R. & Cao, G. 2001 Sardinian natural clinoptilolites for heavy metals and ammonium removal: experimental and modeling. *Chem. Eng. J.* **84**, 275–282.

Doonan, C. J., Tranchemontagne, D. J., Glover, T. G., Hunt, J. R. & Yaghi, O. M. 2010 Exceptional ammonia uptake by a covalent organic framework. *Nat. Chem.* **2**, 235.

Guan, Y. F., Qian, C., Chen, W., Huang, B. C., Wang, Y. J. & Yu, H. Q. 2018 Interaction between humic acid and protein in membrane fouling process: a spectroscopic insight. *Water Res.* **145**, 146–152.

Habibul, N. & Chen, W. 2018 Structural response of humic acid upon binding with lead: a spectroscopic insight. *Sci. Total Environ.* **643**, 479–485.

Halim, A. A., Aziz, H. A., Megat, A. M. J. & Ariffin, K. S. 2010 Comparison study of ammonia and COD adsorption on zeolite, activated carbon and composite materials in landfill leachate treatment. *Desalination* **262**, 31–35.

James, S. L. 2003 Metal-organic frameworks. *Chem. Soc. Rev.* **32**, 276.

Karadag, D., Koc, Y., Turan, M. & Armagan, B. 2006 Removal of ammonium ion from aqueous solution using natural Turkish clinoptilolite. *J. Hazard. Mater.* **136**, 604–609.

Lange, N. A. & Dean, J. A. 2005 *Lange's Handbook of Chemistry[M]*. McGraw-Hill, New York, NY.

Mook, W. T., Chakrabarti, M. H., Aroua, M. K., Khan, G. M. A., Ali, B. S., Islam, M. S. & Hassan, M. A. A. 2012 Removal of total ammonia nitrogen (TAN), nitrate and total organic carbon (TOC) from aquaculture wastewater using electrochemical technology: a review. *Desalination* **285**, 1–13.

Mustafa, S., Nadia, L. H., Rehana, N., Naeem, A. & Samad, H. Y. 1997 Ligands sorption studies on transition metal ion loaded amberlite IRC-50. *Langmuir* **14**, 2378–2384.

Mustafa, S., Nadia, L. H., Rehana, N. A., Naeem, A. & Samad, H. Y. 1998 Ligands sorption studies on transition metal ion loaded amberlite IRC-50. *Langmuir* **14**, 2378–2384.

Peng, C., Chai, L. Y., Tang, C. J., Min, X. B., Song, Y., Duan, C. & Yu, C. 2017 Study on the mechanism of copper-ammonia complex decomposition in struvite formation process and enhanced ammonia and copper removal. *J. Environ. Sci.* **51**, 222.

Saha, D. & Deng, S. 2010 Ammonia adsorption and its effects on framework stability of MOF-5 and MOF-177. *J. Colloid Interf.* **348**, 615–620.

Saltalı, K., Sarı, A. & Aydın, M. 2007 Removal of ammonium ion from aqueous solution by natural Turkish (Yıldızeli) zeolite for environmental quality. *J. Hazard. Mater.* **141**, 258–263.

Sareer, O., Mazahar, S., Akbari, W. M. K. A. & Umar, S. 2015 *Nitrogen Pollution, Plants and Human Health*. Springer, The Netherlands.

Sun, S. L. & Wang, A. Q. 2006 Adsorption properties and mechanism of cross-linked carboxymethyl-chitosan resin with Zn(II) as template ion: react. *Funct. Polym.* **66** (8), 819–826.

Tang, C. J., Zheng, P., Chai, L. Y. & Min, X. B. 2013 Characterization and quantification of anammox start-up in UASB reactors seeded with conventional activated sludge. *Int. Biodeter. Biodegr.* **82**, 141–148.

Tang, C. J., Duan, C. S., Yu, C., Song, Y. X., Chai, L. Y. & Xiao, R. 2017 Removal of nitrogen from wastewaters by anaerobic ammonium oxidation (anammox) using granules in upflow reactors. *Environ. Chem. Lett.* **15**, 1–18.

Vasiliu, S., Bunia, I., Racovita, S. & Neagu, V. 2011 Adsorption of cefotaxime sodium salt on polymer coated ion exchange resin microparticles: kinetics, equilibrium and thermodynamic studies. *Carbohydr. Polym.* **85**, 376–387.

Wang, L., Zhang, H., Lu, C. & Zhao, L. 2014 Ligand exchange on the surface of cadmium telluride quantum dots with fluorosurfactant-capped gold nanoparticles: synthesis characterization and toxicity evaluation. *J. Colloid Interf. Sci.* **413**, 140–146.

Wang, A. H., Zhou, K. G., Liu, X., Liu, F., Zhang, C. & Chen, Q. Z. 2017 Granular tri-metal oxide adsorbent for fluoride uptake: adsorption kinetic and equilibrium studies. *J. Colloid Interf.* **505**, 947–955.

Wirthensohn, T., Waeger, F., Jelinek, L. & Fuchs, W. 2009 Ammonium removal from anaerobic digester effluent by ion exchange. *Water Sci. Technol.* **60**, 201–210.

Yuan, M. H., Chen, Y. H., Tsai, J. Y. & Chang, C. Y. 2016 Ammonia removal from ammonia-rich wastewater by air stripping using a rotating packed bed. *Process Saf. Environ.* **102**, 777–785.

Zhou, C., Wu, Q., Lei, T. & Negulescu, I. I. 2014 Adsorption kinetic and equilibrium studies for methylene blue dye by partially hydrolyzed polyacrylamide/cellulose nanocrystal nanocomposite hydrogels. *Chem. Eng. J.* **251**, 17–24.

Zhou, Z. H., Yuan, J. & Hu, M. 2015 Adsorption of ammonium from aqueous solutions on environmentally friendly barbecue bamboo charcoal: characteristics and kinetic and thermodynamic studies. *Environ. Prog. Sustainable Energy* **34**, 15–12.

Zhu, L. & Ni, J. R. 2009 Improving the ammonium ion uptake onto natural zeolite by using an integrated modification process. *J. Hazard. Mater.* **166**, 52.

First received 4 July 2018; accepted in revised form 5 January 2019. Available online 17 January 2019